ISSN 2504-9593
DOI: 10.5281/zenodo.22026177
https://ijree.com/index.php/publications/article/view/93
Int. J. Renew. Energ & Environ Vol.4 (2), pp 617-641(2026)

PROJECTED HYDROLOGICAL CHANGE IN THE DANO CATCHMENT, BURKINA FASO: IMPLICATIONS OF CLIMATE AND LAND-USE SCENARIOS FOR WATER SCARCITY AND DROUGHT RISK

[1*]Okafor, G. C., [2]Larbi, I., and [2]Limantol, A.
[1]Department of Meteorology and Climate Change, Nigeria Maritime University, Okerenkoko, Delta State
[2]Department of Water Resources and Sustainable Development, School of Sustainable Development, University of Environment and Sustainable Development, Somanya, Ghana.
*Corresponding Author: gloriacokafor@yahoo.com

ABSTRACT
Water resource shortages are a growing concern in the semi-arid Dano catchment, Burkina Faso, where climate and land-use change jointly reshape the ecosystem services local communities depend on. This study uses the Soil and Water Assessment Tool (SWAT), integrating four bias-corrected CORDEX-Africa Regional Climate Models under RCPs 4.5 and 8.5 with two CA-Markov-projected 2050 land-use scenarios, Business-as-Usual (BAU) and Afforestation, to quantify impacts on surface runoff, groundwater/base flow, lateral flow, evapotranspiration (ET), and water yield. Projected land use shows continued forest degradation, agricultural expansion, and settlement growth, with savannah cover declining 8.18% under BAU but recovering 2.13% under Afforestation. Under LULC change alone, water balance components rise modestly: water yield by 0.18-0.28%, runoff by 0.02-3.30%, and ET by 0.21%, while lateral flow falls by up to 1.46% under Afforestation. Under climate change alone, precipitation is projected to fall 20-22% and temperature to rise 1.50-1.70°C (RCP4.5/8.5), driving sharp declines in runoff (up to 77%), groundwater flow (up to 90%), lateral flow (30%), and water yield (64%), alongside a 3.6-3.9% rise in potential evapotranspiration (PET). Combined signals indicate an overall decline in water balance components by 2050, with PET rising 3.2-3.7% even as urban and cropland expansion marginally elevate streamflow. These results reveal a significant association between climate, streamflow, and human land-use pressures, heightening drought and flood risk. Afforestation is identified as key to sustaining future flows, though its benefit is strongly moderated by climate severity. Findings support water managers in pursuing afforestation, erosion control, and water conservation to advance SDGs 6, 13, and 15.
***Keywords**: Water Balance, Surface Runoff, CA-Markov, Afforestation, Ecosystem Function, Agricultural Expansion*

1.0 INTRODUCTION

In recent decades, changes in the environment due to climate change and human activities have become a significant scientific concern, as they affect the availability of water and can lead to hydrological extremes. The altered rainfall patterns in the African region are impacting the quality and quantity of freshwater systems, which has resulted in water security issues. Moreover, the current trend in population growth and water consumption patterns is expected to exceed the sustainable limits of the region's land-based water resources by 2025 [64, 65]. If this situation persists or worsens, additional challenges may arise, as suggested by certain

climate model ensembles used by the IPCC WGI Technical Support Unit (IPCC, 2014) for the region. It is evident from observed and predicted evidence that anthropogenic climate change, manifested as temperature increases and rainfall variability, is influencing the fundamental drivers of the hydrological cycle (Dordai et al., 2026; Li et al., 2026). Consequently, the natural forces resulting from these climatic changes inevitably affect the linkage between the atmosphere and biosphere. This intensification of the hydrological cycle

(Huntington, 2006; Pratap & Markonis, 2022; Akhoudas et al., 2023), along with the overall availability of freshwater and the runoff regimes of most rivers, is being impacted by these human-induced changes. Africa, in particular, has experienced significant and rapid changes in its continental water cycle (Gasse, 2000; Rameshwaran, Bell, Davies, & Kay, 2021). However, increasing human activities such as fossil fuel burning in transportation, mining, and deforestation have contributed to global warming, which is causing climate change. One reason for the growing impact of human activities is the growing global population (Stephenson, Newman, & Mayhew, 2010; Cohen, 2010). The rising population has also led to intensified land use due to elevated demands for agricultural productivity (Duadze, 2004; Andreini, van de Giesen, van Edig, Fosu, & Andah, 2000), dam construction and operation, and logging activities, especially along river basins. As a result, there has been a gradual increase in land-use changes, including urbanisation and agricultural expansion, over the decades to meet human needs. Burkina Faso has experienced severe forest loss due to land-use change, with dense vegetation declining from 37.7% of the landscape in 1990 to just 11.7% in 2022 (Traoré, Ouédraogo, & Zoungrana, 2026). Urban expansion and settlement growth contributed to a 62% increase in built-up areas, driving a 15% reduction in forest cover in regions like the Dano catchment (Okafor, 2019).

Land use and land cover (LULC) change and their dynamics significantly impact the hydrology of a watershed. Hydrological processes are closely linked to the environmental diversity in the area, including factors like topography, vegetation types, soil characteristics, and human-induced influences such as land-use practices. Watersheds undergoing development and changes in land use experience notable shifts in their hydrological behaviour, including modifications to surface properties like evapotranspiration, flood volumes, and runoff components. Moreover, LULC alterations can trigger extreme climate-related events, such as increased flooding risk due to the interaction between climate change, floodplain susceptibility, and flow regulation. Consequently, even minor changes in precipitation can have a significant impact on runoff rates (Grillakis, Koutroulis, & Tsanis, 2011). Prior research has indicated that the Volta River has been significantly impacted by climate change, with vulnerabilities arising from the Inter-Tropical Convergence Zone (ITCZ), the West African monsoon, El Niño Southern Oscillation, and unsustainable land use practices (Barry, Obuobie, Andreini, Andah, & Pluquet, 2005; Awotwi, Kumi, Pe, Yeboah, & Ik, 2015). These factors pose risks to food security and poverty reduction in neighbouring nations. Barry et al. (2005) found that the Volta basin has already experienced notable changes in hydrological patterns, including increased potential evaporation and altered precipitation patterns, exacerbating water resource challenges in the region. Additionally, Andreini, van de Giesen, van Edig, Fosu, & Andah, 2000 Amenuvor, Gao, Li, & Shao, 2020; Abungba, Khare, Pingale, Adjei, Gyam, & Odai, 2020) studies show that in the Volta River Basin, rainfall has declined by about 5-20% in upstream regions since the 1960s, while downstream areas show slight increases; runoff reductions are more severe, with streamflow decreasing by 15–23% in many sub-catchments due to both climate variability and dam regulation. Similarly, Sood, Muthuwatta, & McCartney (2013) projected increased climate variability and a significant 40% decline in river flow, primarily due to reduced rainfall and higher temperatures, particularly toward the end of the century.

Furthermore, LULC change has been associated with adverse consequences, including diminished biodiversity, soil degradation, and restrictions on the capacity of ecosystems to meet human needs, thereby affecting the overall value of hydrological ecosystem services (Yan et al., 2016; Fürst & Flügel, 2015). Alterations in vegetation, whether in terms of type or extent, can bring about modifications in water availability and quality. A global study by Bradshaw, Sodhi, Peh, & Brook (2007) underscores how deforestation escalates the vulnerability to floods and erosion in developing nations. Loss of land cover leads to heightened runoff intensity, resulting in an expansion of the channel network and an increased supply of sediment along the primary network (Tucker & Slingerland, 1997; Muhammed, Nasidi, & Wayayok, 2022; Shree & Kumar, 2023). Similarly, Kundu & Olang (2011), in their analysis of flood events in the Nyando River basin utilizing multi-temporal Landsat images, identified significant increases (16%) in peak runoff levels, particularly in regions experiencing higher deforestation rates.

Numerous studies indicate that land use and land cover changes exert more pronounced effects on hydrological processes at smaller scales (Ahn & Merwade, 2014; Kachholz & Tränckner, 2021; ScienceDirect, 2026; MethodsX, 2026). Nonetheless, the combined impacts of these changes and climate change don't consistently accelerate hydrological processes due to potential offsets (Zhang, Nan, Yu, & Ge, 2015). Understanding the full extent and direction of their interconnected feedback mechanisms remains a complex and incompletely explored area (Wohl, Dwire, Sutfin, Polvi, & Bazan, 2012; Yang, Yang, & Xia, 2021). This knowledge gap is especially critical for smaller catchments, shedding light on how hydrological systems respond to gradual changes over time (Seibert & Van Meerveld, 2016).

Consequently, accurately forecasting the consequences of climate and land use and land cover changes on freshwater availability, flood risks, and erosion rates is a formidable scientific challenge. In response to these considerations, this study's primary objective is to quantitatively assess how water balance components in the Dano Catchment, part of the Black Volta basin, respond to anticipated changes in land use, land cover, and climate by 2050. To achieve this goal, the study outlines specific objectives. First, two land use change scenarios - one representing a business-as-usual scenario (BAU) and the other involving afforestation were developed. These scenarios were developed based on transition probabilities of land use and land cover within the watershed, as determined by the CA-Markov model. Second, the study analyzed climate change signals under two Representative Concentration Pathway (RCP) scenarios. Third, the individual impacts of both land use and climate change on the primary water balance components were simulated. Finally, the study evaluated the combined effects of these factors on streamflow with possible implications in the Dano watershed.

2.0 MATERIALS AND METHODS

2.1 Study Location

The Dano Catchment, covering approximately 582 square kilometres, is a vital part of the expansive Black Volta basin, situated in the southwestern region of Burkina Faso (Figure 1). This basin is a significant component of the larger Volta basin, extending across multiple countries, with 40.2% in north-western Ghana, 46.2% in southwestern Burkina Faso, 3.0% in northeastern Cote d'Ivoire, and 3.1% in southern Mali (Barry et al., 2005; Xavier, 2012). As a focal catchment within the WASCAL Core Research Program, the Dano catchment's geographical coordinates range from latitudes 7°00' to 14°30' North of the equator and longitudes 10°30' to 50°30' West. It plays a crucial role in meeting downstream water resource needs and serves as a pertinent area for studying the effects of climate change on the basin's water resources. The climate in this region is chiefly influenced by the Intertropical Convergence Zone (ITCZ) dynamics in West Africa, further shaped by local orographic factors. This climatic system brings substantial rainfall, primarily induced by convective activity around the ITCZ. The Sudanian savannah climate prevailing in the area leads to varying annual precipitation levels, with the south receiving around 1200 mm per year and the north experiencing lower levels at approximately 500 mm per year. Analyzing data from the Burkina Faso National Meteorological Service between 1970 and 2013 reveals that the region's most significant rainfall occurs over six months, with approximately 80% concentrated between June and September. The region's geological foundation consists of Paleoproterozoic or Precambrian basement rocks, featuring a predominantly flat topography with an average slope of 2.9%. Elevation within the catchment ranges from 256 to 504 meters above sea level. The dominant soil types in the area include *Haplic Plinthosols* and *Cambisols*, with smaller proportions of *Acrisols, Fluvisols, Lixisols, Leptosols, and Gleysols* derived from mid-Palaeozoic-age granite rocks. These soils are known for their structural fragility, rendering them susceptible to degradation under agricultural activities, resulting in reduced fertility and limited water retention. The region's vegetation, characteristic of a semi-arid agroecological zone, predominantly features grass, shrubs, trees, and terrestrial herbaceous and woody plants like the baobab tree (*Adansonia digitata*), néré (*Parkia biglobosa*), shea nut (*Vitellaria paradoxa*), tamarind tree (*Tamarindus indica*), among others. The primary crops cultivated in this area include cereals, millet, maize, rice, cowpea, cotton, groundnuts, potatoes, and yams.

Major soil types in the catchment area are *Haplic Plinthosols* and *Lixisols,* while *Acrisols, Leptosols, Fluvisols,* and *Gleysols* occur in relatively smaller proportions derived from rocks of the mid-Palaeozoic age granite. These soils are distinguished by their high structural fragility, which makes them easily degradable beneath crops, resulting in low fertility and a limited water reserve. The vegetation of the watershed within the semi-arid agroecological zone is dominated by grass, shrubs and trees. Some terrestrial herbaceous plants and woody plants include *Adansonia digitata* (baobab tree), *Parkia biglobosa* (néré), *Vitellaria paradoxa* (shear nut), *Tamarindus indica* (tamarin tree), etc. The main crops include potatoes, millet, cotton, groundnuts and maize.

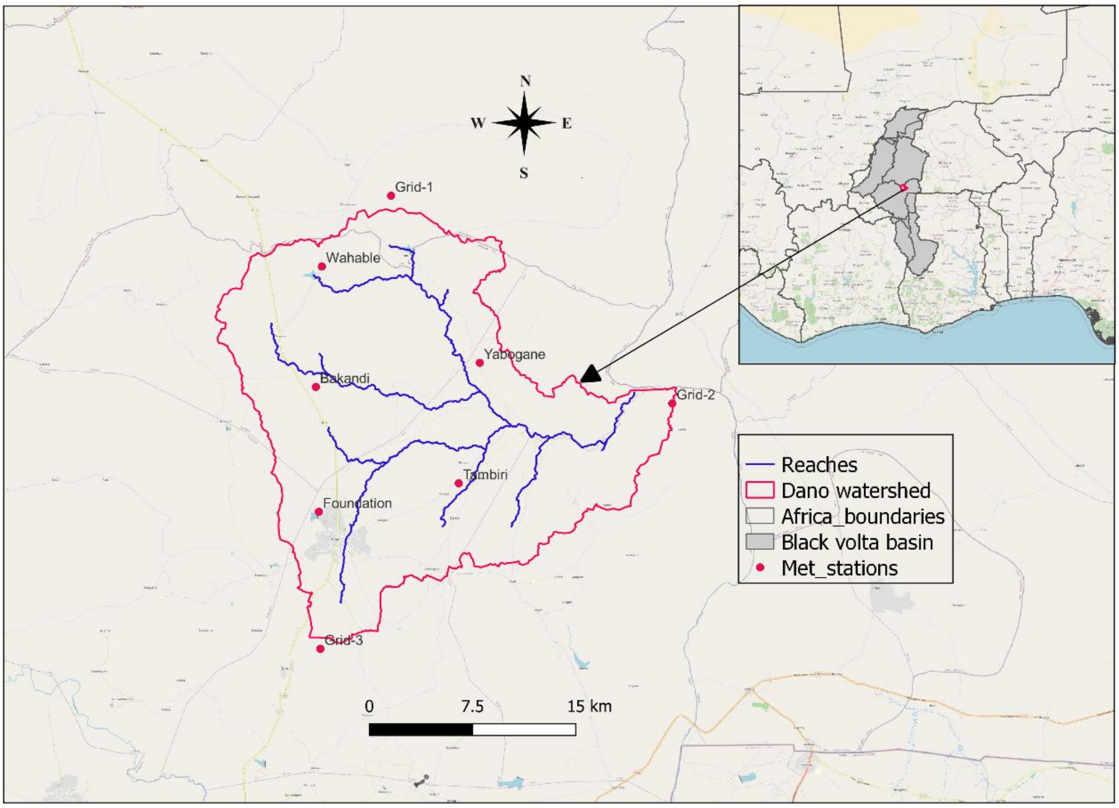

Fig. 1: Dano Watershed in Black Volta Basin, Burkina Faso and the locations of meteorological stations

2.2 Data collection

The details of datasets for this research study are presented under climate and spatial data.

2.2.1 Historical Climate Data And Projections

The study used satellite-based observations of daily rainfall and temperature (minimum and maximum) data provided by the CHIRPS (Climate Hazards Group InfraRed Precipitation with Station data) and ERA5 (ECMWF atmospheric reanalysis of the global climate produced by the Copernicus Climate Change Service (C3S) (Funk et al., 2015; Hersbach et al., 2020). The data covered the period 1990-2016 from five gauge stations distributed in the Dano catchment (Figure 1). Four outputs of Regional Climate Model (RCM) simulations carried out in the framework of the CORDEX-AFRICA were bias-corrected and utilized as climate projections (2020-2049) to run the SWAT model. These RCMs from Swedish Meteorological and Hydrological Institute, Rossby Centre (SMHI); NCC-NorESM1-M-RCA4, CNRM-CERFACS-CNRM-CM5-RCA4, CCCma-CanESM2-RCA4 and Max Planck Institute for Meteorology (CSC); MPI-M-MPI-ESM-LR-REMO2009 are obtainable on the Earth System Grid Federation (ESGF) portal as part of the CORDEX project. The selection of these models was grounded in their compatibility with the specific RCP scenarios, with a particular emphasis on RCP4.5 and RCP8.5. These scenarios were singled out for their superior performance in prior evaluations conducted within the Black Volta basin (Okafor, Annor, Odai, & Agyekum, 2019). In the case of RCP4.5, this scenario outlines a trajectory where carbon dioxide emissions are anticipated to commence a decline around 2045, to reach approximately half of the 2050 emission levels by the year 2100. On the other hand, RCP8.5 depicts a scenario in which emissions are expected to continuously escalate throughout the entirety of the 21st century, aligning with projections by the Intergovernmental Panel on Climate Change (IPCC). These are comparable to the SRES B1 scenario and A2/A1FI, respectively.

2.2.2 Catchment Flow Data

Daily observed streamflow data available from 2013 to 2016 were obtained at the Batiara gauging station downstream of the watershed and used to calibrate and validate the SWAT model.

2.2.3 Spatial Data

The study utilized geospatial data, including the Digital Elevation Model (DEM), land use classifications, soil attributes, and slope information, as presented in Figure 2. Initially, a high-resolution Shuttle Radar Topography Mission (SRTM) DEM with a 30-meter resolution was obtained from the United States Geological Survey (USGS) website (http://earthexplorer.usgs.gov/) to delineate the watershed's boundaries and acquire essential topographical and morphometric characteristics of the land surface terrain (Figure 2a). Subsequently, data related to slope steepness was extracted from the DEM and categorized into two segments: 0-10% and 10-99%, covering 80.07% and 19.82% of the entire watershed area, respectively. The classified LULC of the Dano watershed (Okafor, Annor, Odai, & Larbi, 2019) with five categories based on the SWAT code was used. The watershed encompassed water bodies (0.10%), forested regions (35.94%), urban areas (2.68%), croplands (52.05%), and grasslands (9.12%), as illustrated in Figure 2b.

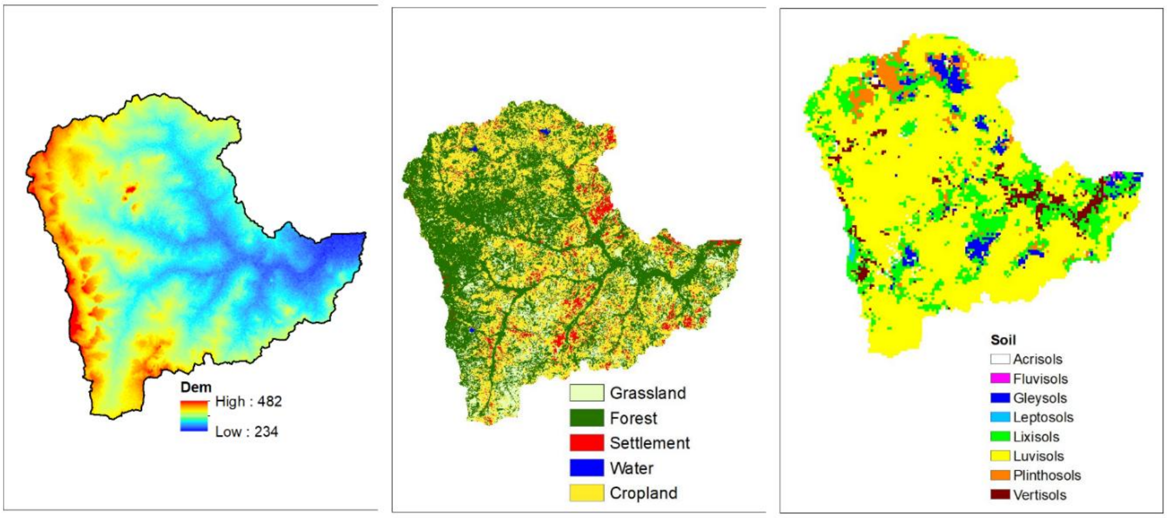

Figure 2: Spatial data inputs a. Digital Elevation Model b. Land-use (2016) and c. Soil types in the Dano Catchment.

Regarding soil-related data, a soil map was obtained in a raster format with a spatial resolution of 250 meters from SoilGrids (Hengl et al., 2017). The dataset for soil properties was derived from the comprehensive work conducted by Forkuor, Hounkpatin, Welp, & Thiel (2017) focusing on soil property mapping within the Dano watershed. The soil classification, as presented in Figure 2c, identified the presence of eight distinct soil types, displaying variations within the sub-basins. Notably, luvisols (69%), lixisols (18%), vertisols (4%), and plinthosols (4%) were the dominant soil classes in the area.

2.3 ECO-HYDROLOGICAL MODELLING

This study's methodology included land-use change modelling, climate projections, and SWAT eco-hydrological modelling (Figure 3). The CA–Markov model was utilized to estimate future land-use change, while climate models were bias-corrected for projected climate change signals in 2050. Afterwards, the projected land use and climate change scenarios were utilized to simulate streamflow in the SWAT model for the Dano watershed.

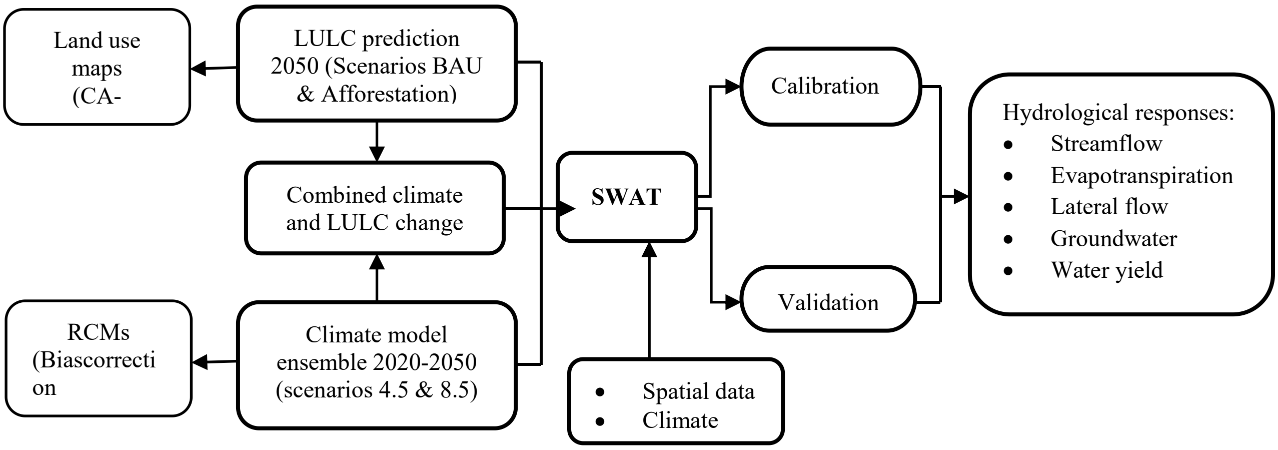

Figure 3: Graphical summary of steps used in the eco-hydrological analysis using the SWAT model

2.3.1 Land-use change and scenario modelling (CA-Markov)

The research involved projecting land use patterns for the year 2050 using a hybrid cellular automata (CA)-Markov model, established by Nazzal, El-Emary, & Najim (2008) as previously detailed in Okafor et al. (2019) for the Dano catchment. The CA-Markov model is particularly suited for representing spatiotemporal changes in landscape configurations and has garnered widespread acceptance in various scientific disciplines (Mukhopadhaya, 2016). The modelling process encompassed distinct stages, including the identification of changes within the land use and land cover (LULC) classes, the modelling of transition potentials, the determination of driving factors influencing transitions between two observed time points, change prediction, and model validation. Key drivers of land use changes integrated into the modelling comprised of slope characteristics, settlement patterns, elevation attributes, as well as proximity to roadways and rivers. To gauge the model's efficacy, initial assessments utilized LULC data from 1990 and 2000 to predict the LULC status in 2010. Once the model demonstrated its reliability, it was subsequently applied to project land use scenarios for 2050, using the 1990 and 2016 maps as baseline references. Two distinctive scenarios were devised: the Business as Usual (BAU) scenario, which relied on historical land use transformations from 1990 to 2016, considering transition probabilities, with a particular emphasis on primary change categories encompassing areas exceeding 5000 hectares to manage transition complexity within the modeling process. The Markov model's predictions played a crucial role in defining the drivers for the catchment area. The second scenario, denoted as Afforestation, was characterized by adjustments to the probability matrices governing forest, farmland, and grassland categories. Notably, this scenario entailed an overall increase in the Annual Land

Use/Cover Change Rate (ALUCR) with a specific focus on augmenting the rate of forest conversion, as elaborated in Table 1.

Table 1: Land cover change scenarios.

Scenario	LULC	Description
Baseline	2016	LULC classified areas for water, settlement, forest, cropland and grassland
BAU (Business as usual)	2050	The pattern of LULC transitions from 1990 to 2016 (expansion of cropland at the expense of grassland and forests).
Afforestation	2050	Increase forest by 15% (ALUCR*30) in the future by limiting cropland expansion.

2.3.2 Bias-correction of Climate Models and change signals

Prior to climate projection, bias correction was applied to each Regional Climate Model (RCM) using satellite-based observations gathered from gauge locations. The empirical quantile mapping technique, also known as non-parametric distributive mapping, was used to statistically correct the temperature and precipitation results. This correction method was chosen because of its improved performance in comparison to competing methods discussed in (Gudmundsson, Bremnes, Haugen, & Engen-Skaugen, 2012) and (Teutschbein & Seibert, 2012) over the catchment. The raw simulated climate change signals are also preserved via the quantile mapping technique (Cannon, Sobie, & Murdock, 2015). This method's goal is to rectify the output of the RCMs for any inherent biases that are present. A minimum Nash–Sutcliffe efficiency (NSE) of 0.99 and graphical comparison were employed to assess the agreement between the observed and the individual bias-corrected RCM simulation data. The RCMs and their ensemble displayed a commendable alignment with observed data for both rainfall and temperature (Figure 4). This signifies that the initial discrepancies inherent in the unprocessed RCM outputs were removed through the implementation of the distributive mapping technique. Consequently, the adjusted RCMs can be deemed as dependable resources for scrutinizing the potential consequences of climate change within the Dano catchment.

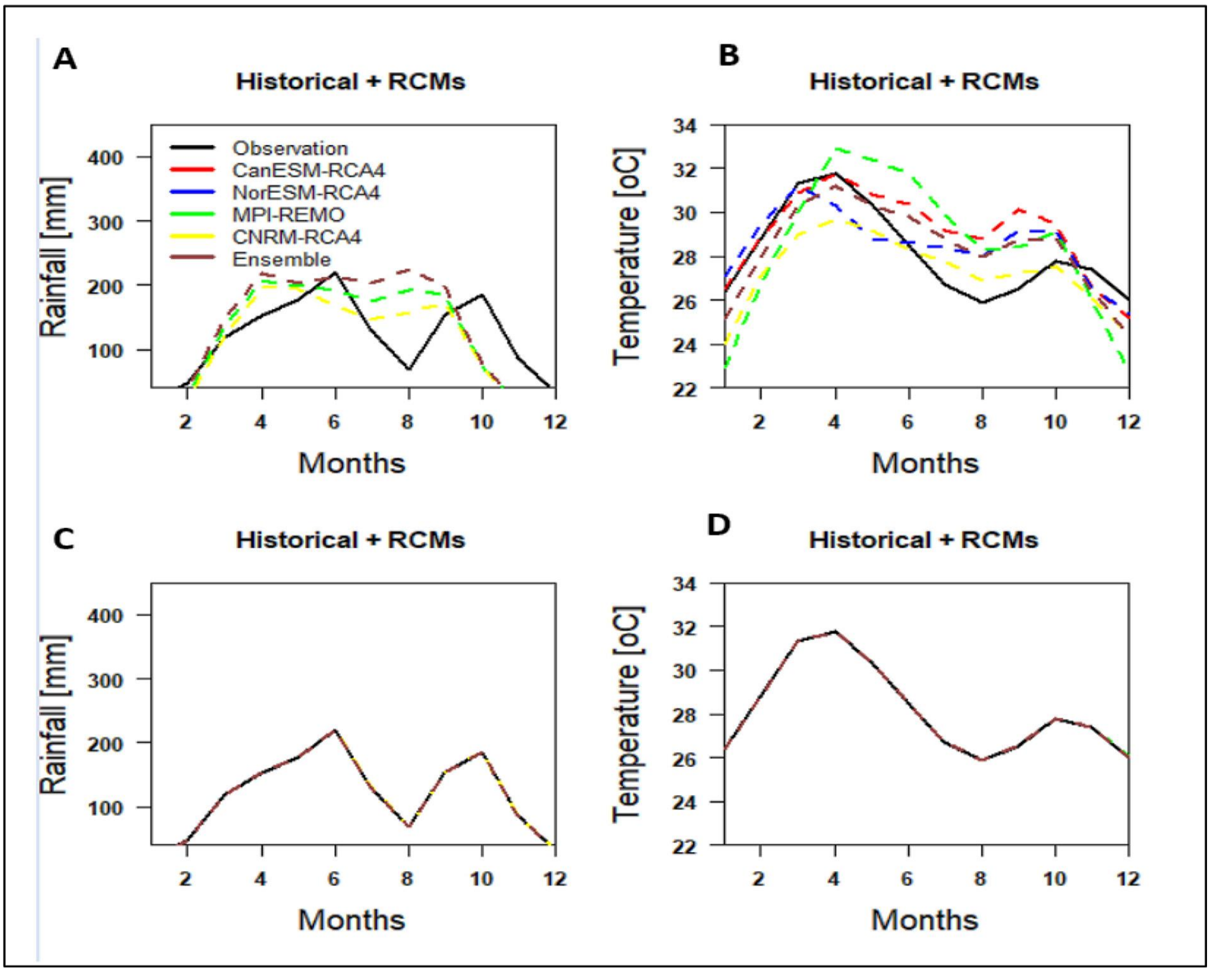

Figure 4: Comparison between monthly (1981–2005) precipitation and temperature of the observed and the RCMs. *A and B show before bias correction while C and D indicate after bias correction*.

Subsequently, the expected climate change signals across the Dano watershed were examined by means of the ensemble mean derived from the four RCMs. By lowering uncertainty, this strategy seeks to increase confidence in upcoming climate change estimates (Luhunga, Botai, & Kahimba, 2016). Evaluations of precipitation and temperature were made for the historical period from 1990 to 2016 and projections for the 2020–2049 time frame under the RCP4.5 and 8.5 scenarios. By deducting the mean values of the observed historical period from the mean values of the future period, the changes in mean climatologies for precipitation and temperature were determined. Additionally, the Student's t-test with a 95% confidence level was used to evaluate the statistical significance of the climate change signal.

2.3.3 Hydrological Modelling in SWAT

The SWAT eco-hydrological model was created to simulate, over an extended period of time, the hydrological response to a variety of scenarios, including variations in weather, soil conditions, and land use (Setegn, Srinivasan, & Dargahi, 2008; Zhang, Hu, Wang, & Ai, 2017; Xu, Zhang, Ran, & Tian, 2013; Haleem et al., 2022). SWAT was utilized in the current evaluation to model runoff's response to potential changes in the climate and in land use. Preparing the data, sub-basin discretization, and hydrological parts (HRU) definition are the stages that are involved. Generally, the model divides the watershed into multiple sub-basins, singly comprised of one or several small HRUs with the use of spatial datasets described earlier. The QSWAT - Quantum GIS interface and associated parameterization were used in the model configuration. This setup involved utilizing the DEM for flow direction and the stream network, and subsequently, the watershed was subdivided into 13 distinct sub-basins. Furthermore, sub-basins were delineated into 190 HRUs based on the Land-use/Soil/Slope threshold 9/5/10 percentages. SWAT, like all physically based models, uses a variety of numerical algorithms to represent energy equilibrium and water movement in the watershed. The laws of mass, momentum, and energy conservation serve as the foundation for the equations (Arnold et al., 2012). The Soil Conservation Service Curve Number SCS CN (SCS-USDA, 1972) was adopted for the estimation of surface runoff. The Hargreaves technique, with the advantage of less stringent input data needs, was employed to calculate evapotranspiration. Finally, the streamflow was routed using the variable storage approach in each sub-basin and contributed to the Network River, then incorporated into the outlet of the watershed. A more detailed and detailed description of SWAT is available (Winchell, Srinivasan, Di Luzio, & Arnold, 2010), as this assessment is limited to the most relevant aspects related to the hydrology component, which is the main focus of attention. SWAT's simulation of the hydrologic cycle is based on the water balance equation shown.

$$SW_t = SW_0 + \sum_{i=1}^{t} \left(Pr_{day} - Q_{surf} - Q_{gw} - ET_a - Perc\right) \qquad (1)$$

where SW_t is the final soil water content, mm; SW_0 is the initial soil water content of the ith day, mm; t is the time, days; Pr_{day} is the precipitation amount of the ith day, mm; Q_{surf} is the surface runoff of day i, mm; Q_{gw} indicates the return flow amount on day i, mm; ET_a indicates the amount of evapotranspiration on day i, mm; and $Perc$ indicates the amount of water entering the vadose zone from the soil profile on day i, mm.

The simulation started from 1990 to 2016 and had the initial 3 years skipped as the warm-up period to reduce the strange initial conditions and also to maximize the simulation. Daily climate inputs were provided for the stated period to obtain process parameters for the whole catchment area.

2.3.4 SWAT Model Calibration and Performance Evaluation

Calibration (manual and automatic techniques) and validation were performed to optimize model performance. Automatic calibration entailed parameterization and sensitivity analysis, utilizing the Sequential Uncertainty Fitting (SUFI-2) algorithm within the SWAT-CUP program. This approach accounted for various uncertainties related to model conceptualization, parameters, and input data, including climate information, all within the framework of 95% prediction uncertainty (95PPU). Additionally, the R-factor was employed to gauge the effectiveness of calibration and uncertainty analysis.

Four comprehensive measures of model performance were computed in this study. These included the Nash-Sutcliffe model efficiency (NSE), which assesses the agreement between observed data and the best simulation. The coefficient of determination (R^2), Percent Bias (PBIAS) and Kling–Gupta efficiency (KGE) were also utilized to evaluate the degree of correspondence between the model's best simulation and observed discharge data. The KGE, specifically, offers insights into the relative significance of variability, correlation and bias, (Roy, He, Lin, Beck, Castro, &

Wood, 2020). Calibration was conducted from 2014 to 2015, while validation was carried out in 2016 using data from the Batiara gauge station, which provided a consistent daily discharge record spanning four years. Subsequently, the validated model was employed to project future simulations of water balance components.

2.3.4 Exploring the Hydrological Consequences of Climate and LULC Changes

Gaining a deeper insight into how two drivers, climate and LULC change, affect watershed hydrological ecosystems is essential for the long-term planning and sustainable management of water resources. To realize how the Dano catchment responds to changes in climate and land use/land cover, we employed three distinct assessment methods: 1) Evaluating the isolated impact of LULC changes, 2) Investigating the sole influence of climate change, and 3) Assessing the combined effects of climate and LULC changes on the key components of the catchment's water balance.

The classified data from 2016 served as the baseline for the study, while two projected land use and land cover (LULC) mapping scenarios for 2050 were utilized to investigate future hydrologic implications. The "fixing-changing method" was employed, which involved modifying either the climatic or the LULC scenarios while keeping other variables constant. For future assessments, the study considered the LULC maps for two scenarios: one representing business-as-usual and the other focusing on afforestation in 2050, along with the multimodel ensemble mean of future climate predictions (2020-2049) under Representative Concentration Pathways (RCPs) 4.5 and 8.5. The Soil and Water Assessment Tool (SWAT) model (Figure 3) was utilized to simulate future surface flow under these scenarios, and the resulting hydrological components (such as actual and potential ET, water yield, streamflow, groundwater flow and lateral flow) were compared on an annual average basis.

3.0 RESULTS AND DISCUSSION

3.1 Land Use Change Analysis and Projection

The land use proportions and change analysis of the Dano watershed between 1990 and 2016 are presented. The results reveal that forest degradation, agricultural land expansion, settlement growth, and more stable grassland occurred (Figure 5).

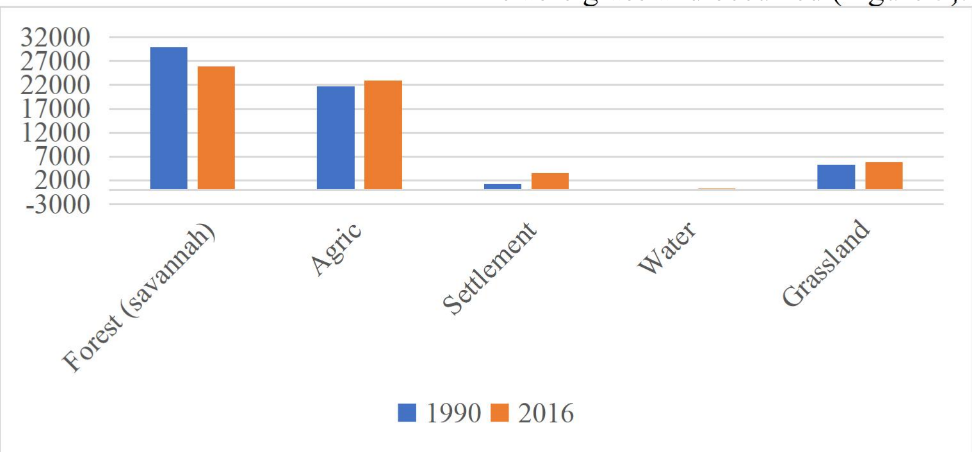

Figure 5: Proportions of LULC Types in Dano Catchment

Table 2: Annual Rate of Change in LULC from 1990 to 2016

Class (Area change)	1990-2016		
	ha	%.yr	%*30
Forest (savannah)	-4093.52	-0.52	**-15.75***
Agric	1209.1	0.21	6.43
Settlement	2364.16	7.61	228.18
Water	219.01	11.76	352.74
Grassland	494.12	0.36	10.78

scenario rate of increase

Forest lost approx.14% from 1990 (29997.99 ha) to 2016 (25904.47ha) of its overall area with a 0.52%/yr consistent change. While agriculture, settlement, water and grassland rose respectively at annual rates of 0.21, 7.6, 11.7 and 0.3 %. To further buttress this change detection and emphasize the significance of the study's LULC focus, the CA-Markov model's determination of the LULC transition probability matrices in the Dano watershed is shown in Table 3. The matrix shows the transition rates as well as quantitatively explains how LULC types are converted. The diagonal values in the matrices indicate the likelihood that each LULC class will remain the same, but the off-diagonal values indicate the likelihood that a class will change. For any 26 years (starting from 1990), we therefore expect 47.87% of forest to persist and 37.86, 5.14, 0.6%, and 9.06% to change, respectively, to agriculture, settlement, water and grassland, with no reversion back to forest. Similarly, 41.85% of cropland will persist, and 42.68, 6.75, 0.15%, and 8.56% will change to forest, settlement, water and grassland, respectively.

Table 3: Probabilities of LULC transitions in the Dano Catchment represented by a Markov chain matrix

Period: from–to	LULC	Forest	Cropland	Settlement	Water	Grassland
1990-2016	Forest	**0.4787**	0.3786	0.0514	0.0006	0.0906
	Cropland	0.4268	**0.4185**	0.0675	0.0015	0.0856
	Settlement	0.3573	0.4777	**0.0908**	0.0014	0.0727
	Water	0.3609	0.1438	0.0529	**0.4214**	0.0210
	Grassland	0.4895	0.3426	0.0385	0.0007	**0.1287**

In the land change model, the most significant transitions between 1990 and 2016 were from forest to all other classes, including water, grassland, settlement, and largely to agriculture, totalling 5023 ha; hence, considered as the major transition (i.e. agricultural land area increases and forest decreases). This is because urban areas only make up less than 7% of the watershed. All other classes transition to settlement (column-wise). The main determinant of the shift in land use was settlement, which was followed by proximity to rivers and the road factor. This suggests that in order to meet fundamental demands for survival, nearby habitation sites have been removed for the production of food.

The projection of future LULC changes in the year 2050 (Figure 6) was carried out by utilizing the 1990 and 2016 maps, applying a sub-model test-implemented calibration. The analysis predicts that under a business-as-usual scenario (BAU), the forested area is expected to decrease by 8.18%, transitioning from 46.72% to 38.54%. Simultaneously, cropland is anticipated to expand from 38.51% to 46.69%. In contrast, the afforestation scenario foresees a 2.13% increase in forest cover compared to the conditions in 2016.

In general, based on the results, it is anticipated that there will be an escalation of land degradation, indicating changes in the ecosystem, particularly in the water balance of the catchment, which will likely result in modifications to the hydrological patterns. In the scenario representing BAU, an expansion of agricultural activities may lead to a further reduction in savannah land cover, estimated at approximately 8.18%. This change has the potential to disrupt the regulation of runoff and increase sedimentation. On the other hand, in the afforestation scenario, there is a projected increase in forested savannah by approximately 2.13% when compared to the baseline conditions. These findings are consistent with previous studies conducted by scholars who have investigated land use in African savannah regions (Knauer, Gessner, Fensholt, Forkuor, & Kuenzer, 2017; Sanogo, Dayamba, Renaud, & Feurer, 2022; Tripathi, Woollen, Carvalho, Parr, & Ryan, 2021; Adenle, Eckert, Adedeji, Ellison, & Speranza, 2020). Alongside deforestation, the expansion of agricultural activities can also lead to alterations in the structure of the ecosystem. Thus, considering the projected rapid population growth in Burkina Faso, at a rate exceeding 3% annually (INSD, 2020), the results highlight the importance of strategic land use planning and the implementation of mitigation policies within the catchment to address the potential loss of natural land cover.

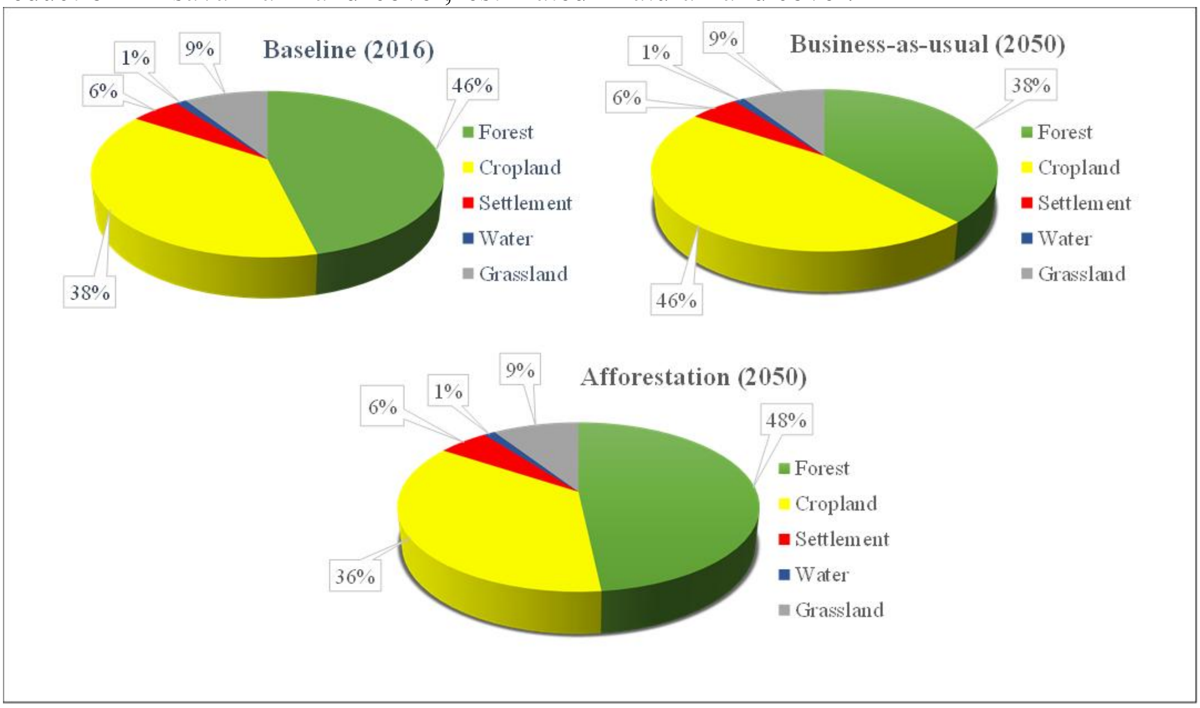

Figure 6: Area statistics of baseline and future periods of land use developed in this study.

3.2 Projected Climate Change

The anticipated climate change signal for the 2050s, as derived from the ensemble mean of the RCMs relative to the base period (1990-2016), is illustrated in Figures 7a and 7b. In the coming decades, the catchment is poised for a noticeable reduction in average precipitation, estimated at approximately 20% and 22% under the RCPs 4.5 and 8.5 scenarios, respectively. Furthermore, temperature changes indicate a significant warming trend, with projections ranging from 1.4°C to 1.6°C by mid-century. This perceptible temperature increase is expected to occur at a rate of 0.14°C to 0.16°C per decade, potentially leading to an increase in PET.

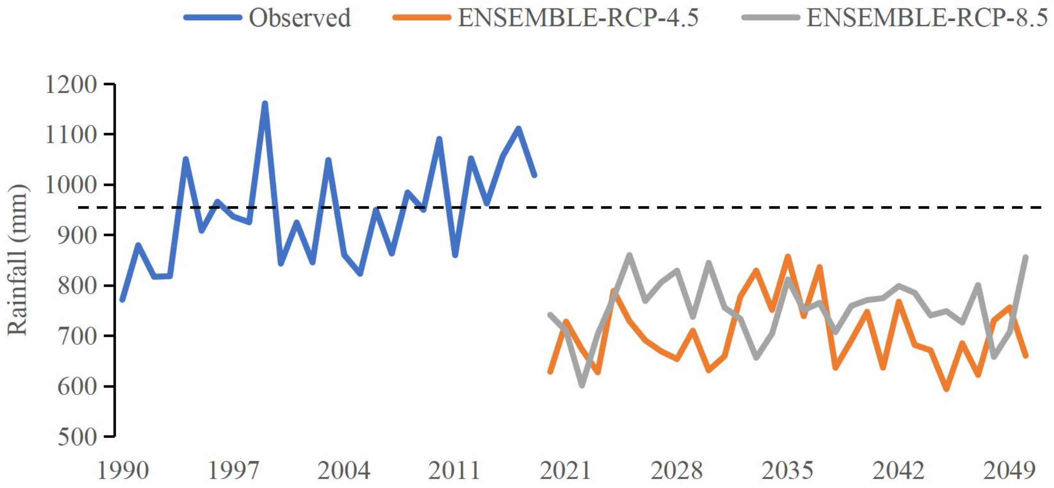

Figure 7a: The anticipated variations in annual precipitation (mm) between 2020 and 2049 in comparison to the baseline (observed) period of 1990–2016. *NB: the dashed horizontal lines show the average observation from 1990 to 2016.*

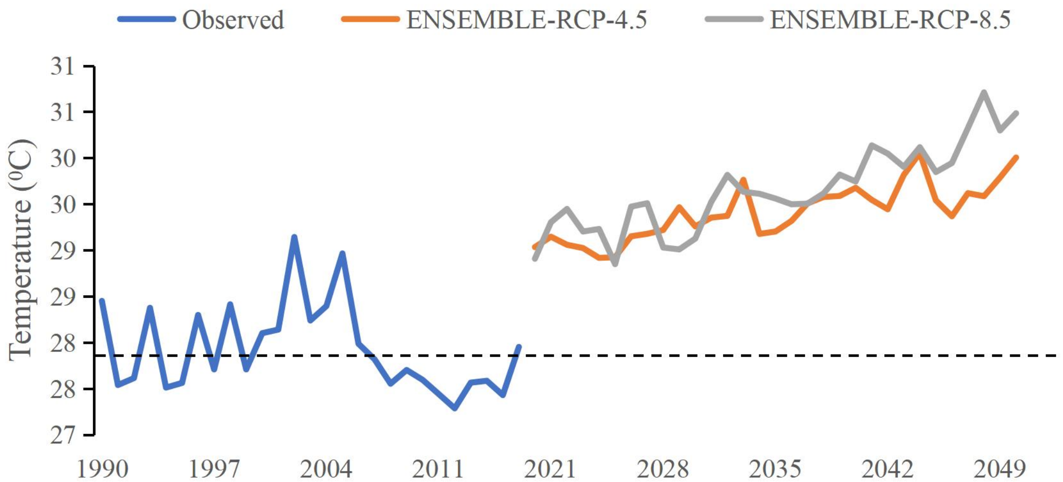

Figure 7b: Future predicted variations in annual temperature (0C) from the baseline (observed) period of 1990–2016 to 2020–2049. *NB: The dashed horizontal lines show the average observation from 1990 to 2016.*

The projected climate changes align with the findings outlined in AR5(IPCC, 2014) for the upcoming 2050s in the specific region. The RCM simulations are in concurrence with prior assessments conducted within the West African domain, indicating a substantial 25% reduction in rainfall (Bossa, Diekkrüger, & Agbossou, 2014; Darko, Adjei, Appiah-Adjei, Obuobie, Asmah, & Odai, 2018). These projections also support the research conducted by (Aziz & Obuobie, 2017), who observed significant warming and shifts in mean precipitation levels, ranging from approximately -23% to -33%, specifically under RCPs 4.5 and 8.5, respectively, by the conclusion of the 21st century over the Black Volta basin. The implication is the pressing necessity for the implementation of adaptation strategies, emphasizing their critical role in mitigating the risks associated with reduced rainfall on both water resources and human well-being. Moreover, recent extreme weather events like droughts and floods vividly demonstrate the vulnerability of terrestrial ecosystems, communities, and economies to the impacts of climate change.

3.3 Sensitive SWAT Parameters, Calibration And Validation Results

The SWAT model was calibrated, and a sensitivity analysis was conducted on 13 flow parameters to assess their impact on the model's flow component and optimize them for the objective function. Among these parameters, five were identified as particularly influential, as evidenced by their remarkably low p-values and high absolute T-stat values. These key parameters—GWQMN (Threshold depth of water for return flow in shallow aquifer, mm), ESCO (Soil evaporation compensation factor), GW_DELAY (Groundwater delay in days), CN2 (Curve number for different landcover), and EPCO (Plant uptake compensation factor)—are closely tied to both soil (groundwater) and land cover (streamflow) characteristics in the catchment. Therefore, these parameters necessitate special attention and effective land management practices, especially in soil erosion control efforts. The hydrograph in Figure 8 visually contrasts the observed and simulated flow during both the calibration and validation periods. Table 4 provides the indices utilized to assess the accuracy of the simulation and the appropriateness of the model parameters. Optimal values for R^2 and NSE are 1, while for PBIAS, it is 0. The achieved values include NSE above 0.5, R^2 surpassing 0.9, and PBIAS below 25%. The assessment of model performance suggests that the simulation results are deemed satisfactory.

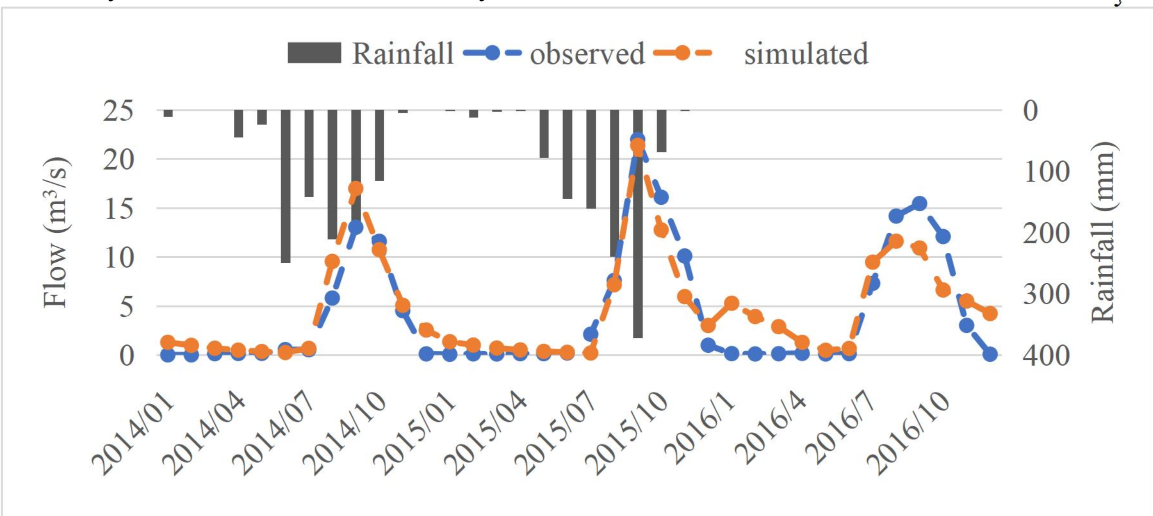

Figure 8: Hydrograph illustrating the monthly average of the simulated and observed streamflow for the SWAT model's validation (2016) and calibration (2014–2015).

Table 4: SWAT Model performance statistics for the calibration and validation periods

Period	Performance Statistics				Uncertainty
	NSE	**R^2**	**KGE**	**PBIAS**	**r-factor**
Calibration	0.92	0.94	0.79	-20.4	0.78
Validation	0.87	0.92	0.71	5.0	0.53

Figure 8 illustrates a strong correlation between rainfall and streamflow, indicating elevated runoff during months with increased precipitation. The simulated discharge consistently aligns with the observed pattern during the calibration, with only a minor underestimation of peak flow observed during validation. This is due to the nature of the catchment (topography and 46% cropland) as the streamflow occurred mostly during the rainy season by means of overbank flow. Nevertheless, the results demonstrate that the SWAT model effectively replicates the catchment's characteristics. The evaluation criteria proposed by Moriasi, Arnold, Van Liew, Bingner, Harmel, & Veith (2007) affirm the model's competence, affirming its suitability for evaluating hydrological impacts resulting from climate and land use changes in the watershed spanning from 1990 to 2050.

3.4 Dano Catchment's Response to Potential LULC and Climate Changes

3.4.1 Impact of LULC change

After validating the SWAT model, the study assessed the impact of LULC changes on watershed hydrology. The predicted 2050s land use data for both business-as-usual (BAU) and Afforestation scenarios (Figure 5) were integrated into the calibrated SWAT model, with other parameters held constant, to simulate streamflow. Subsequently, the annual water balance components, encompassing actual and potential evapotranspiration (ETa and PET), surface runoff, lateral flow (LATQ), groundwater flow (GWQ), and water yield, were analyzed (Table 5). In the BAU scenario, marked by increased cultivated land and settlement area and reduced Savannah, a marginal 0.02% rise in average annual surface runoff and a 0.21% increase in evapotranspiration from the baseline were noted. Conversely, lateral flow decreased, and PET showed no change. Equally, the afforestation scenario, with expanded forest cover, led to a 3.3% increase in runoff, a 0.28% rise in water yield, and contributed to an upturn in potential evapotranspiration. The small increase in runoff can be attributed to more cropland/settlement areas (urbanisation). The existence of deep-rooted woods in the catchment is able to use deep water reservoirs during the dry season, reducing baseflows. This result implies increasing soil erosion and soil compaction associated with logging, deforestation, etc. Therefore, there is a need for appropriate soil water management practices in the catchment.

Table 5: Summary of average annual baseline and projected (the 2050s) hydrological change

Period	Precipitation (mm)	Runoff (m^3/s)	ETa (mm)	PET (mm)	GWQ (mm)	LATQ (mm)	Water Yield (mm)
Baseline	958.76	90.1	674.3	1952.1	49	48.02	214.1
Rainy season (Apr-Oct)	943.3	90.1	576.0		-	37.8	156.6
Dry season (Nov - Mar)	15.4	0.0	98.3		-	10.3	57.5
Land-use scenarios				**Percentage changes**			
BAU	0.00	0.02	0.21	-	1.59	-0.40	0.18
Afforestation	0.00	3.30	0.28	-	1.10	-1.46	0.28
Climate scenarios				**Percentage changes**			
Scenario 4.5	-22.2	-77.9	-8.6	3.6	-90.8	-28.4	-63.4
Scenario 8.5	-20.5	-76.7	-11.1	3.9	-84.2	-30.1	-64.5

3.4.2 Impact of Climate Change

The hydrological cycle, influenced by climate factors such as energy (min and max temperature) and moisture (precipitation), plays a crucial role in shaping environmental processes. Employing two prospective climate change scenarios (RCPs 4.5 & 8.5), the SWAT model was utilized to forecast alterations in streamflow within the Dano catchment. The examination of the catchment revealed a noteworthy decline in mean annual precipitation (approx. 20%) as a consequence of climate change impacts, leading to a substantial reduction in runoff for both climate scenarios (refer to Table 6). This decline was predominantly attributed to reductions in Evapotranspiration (ETa), which exhibited disparities compared to the reductions in surface runoff. Additionally, an anticipated temperature rise of approximately 1.50°C in both scenarios, as projected by the climate model ensemble, is expected to result in a respective increase in PET by 3.6% and 3.9%, shifting from 1952.1 mm to 2021.9 mm and 2028.7 mm. Similarly, GWQ, LATQ and water yield show decreases. The Dano catchment will face water scarcity and drought as a result of future decreases in water balance components caused by climate change. As a result, adaptation strategies to build resilience to the influence of climate change on the hydrology of the Dano basin are required.

3.4.3 Future Climate and LULC Change's Combined Effects on key hydrological components

To enhance our understanding of the intertwined impacts of climate change and LULC changes on the catchment's hydrology, scenarios involving simultaneous alterations in climate variables (temperature and rainfall) and predicted LULC changes were considered. The outcomes are depicted in Figure 9, presenting the response of the water balance components within the basin under the combined scenarios for the 2050s, expressed as relative percentage changes compared to the baseline conditions. As indicated by the model results, PET experienced a slight increase ranging from 3.2% to 3.7%, leading to a reduction in runoff by 72% to 77%, along with changes in other flow components.

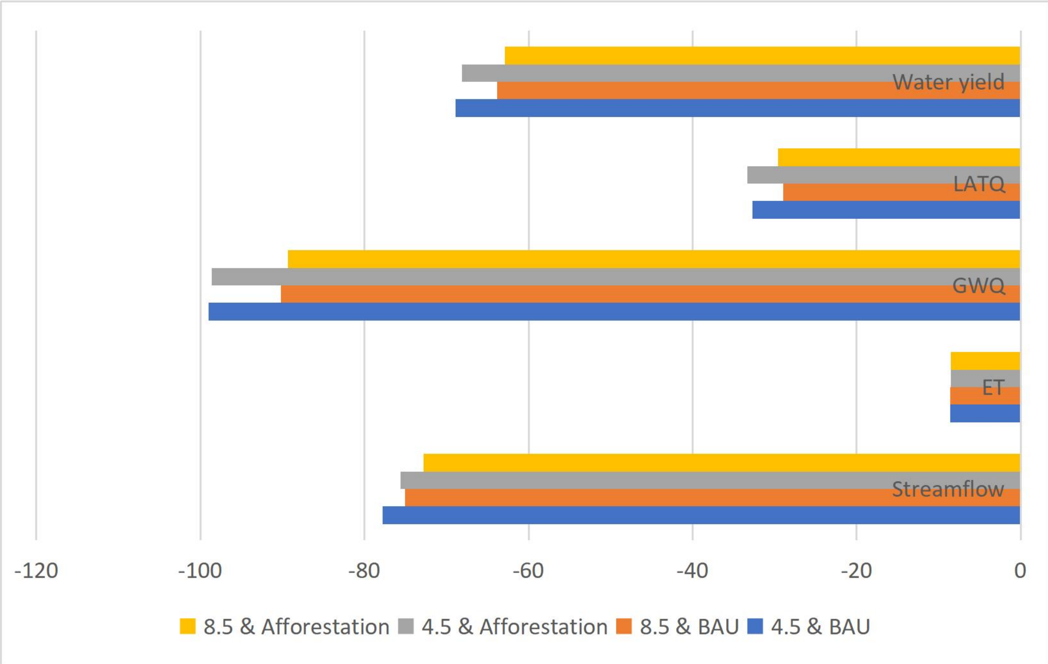

Figure 9: Percentage changes in the hydrological components between 1990 and 2016 in the Dano catchment under several scenarios of coupled climate and LULC change.

3.5 Hydrological implications in Dano watershed due to changes in LULC and climate

The projected land-use impact scenario, characterized by reduced forest cover and the expansion of cropland and settlements from 2020 to 2050 under Business-as-Usual, resulted in a slight augmentation of average annual flow, particularly during the rainy season (April to May), accompanied by elevated temperatures. However, the existing imbalance between Evapotranspiration (ETa) and Potential Evapotranspiration (PET), attributed to inadequate soil water storage due to insufficient precipitation, persisted. Consequently, the intensified evapotranspiration resulting from temperature increases exhibited minimal influence on streamflow. The study underscores the dominance of climate variables over land-use changes, especially with the Hargreaves method utilized for estimating evapotranspiration, where even marginal alterations in precipitation exerted substantial impacts on surface runoff. This sensitivity is vividly illustrated by a notable 99% difference in runoff between rainy and dry seasons, emphasizing the profound influence of precipitation on discharge, as detailed in Table 6. Equally, GWQ, LATQ and water yield decreases are mainly attributed to LULC change and high carbon dioxide emissions occurring during the projected period, signifying a significant impact on groundwater resources in the near future.

This study's findings align with those of previous researchers. The decrease in annual streamflow associated with precipitation, reflecting climate change impacts, is consistent with the reported rainfall decline in Sudanian regions (Descroix et al., 2009). Similarly, Ibrahim, Karambiri, & Polcher (2015) noted a comparable decrease in rainfall and runoff in Burkina Faso's Nakambe basin, attributing it to reduced rainfall frequency and intensity, as evidenced by extreme event analysis (Okafor, Larbi, Chukwuma, Nyamekye, Limantol, & Dotse, 2021). Notably, the study establishes that LULC changes led to increased streamflow despite declining rainfall, supporting the hypothesis that Sudanian catchments, particularly those with dominant sedimentary geology, are more responsive to LULC changes (Descroix et al., 2009). The afforestation scenario resulted in higher runoff, indicating potential factors such as increased evapotranspiration or reduced soil water-holding capacity (Mahe, 2006). This finding aligns with Roudier, Ducharne, & Feyen (2014), who associated streamflow changes with precipitation and, to some extent, potential evapotranspiration in their West Africa-focused review of climate change impacts on runoff.

These investigations (Yira, Diekkrüger, Steup, & Bossa, 2016; Bossa, Diekkrüger, & Agbossou, 2014) have consistently identified evapotranspiration as the predominant factor, comprising 80% of the water balance in the Sudanian zone, a pattern mirrored in our present study. Cornelissen, Diekkrüger, & Giertz (2013) observed a PET increase of 5-14% in scenarios A1B and B1, employing four hydrological models within a catchment akin to our study area. The notable decline in ET can be attributed to persistently arid soils (limited water-holding capacity), potentially initiating a feedback loop impacting climate. This declining trend in ET signifies a diminished local water cycle over the catchment, diverting more energy to sensible heat rather than latent heat, thereby amplifying surface warming and strengthening land-atmosphere interactions (Yang, Zhang, Ran, & Tian, 2016). Furthermore, land cover change significantly alters evapotranspiration, especially when natural vegetation is converted to cropland and settlements. The decrease in ET, influenced by land cover changes, aligns with Dias, Macedo, Costa, Coe, & Neill (2015) findings, illustrating that the transformation of natural vegetation into agriculture substantially alters ET in small catchments, as observed in the Dano watershed.

The combined changes in LULC and climate in the near future resulted in decreasing water balance components, and Ashraf, Ali, Shrestha, Hafeez, Moiz, Sheikh (2022) have reported consequent impacts on groundwater resources. The declining groundwater may be due to changing rainfall patterns, dry spells, an upsurge in water demand and, particularly, limited recharge. Overall, the diminished availability of freshwater resulting from climate change, principally due to reduced precipitation, is somewhat exacerbated by the expansion of agriculture. Adopting sustainable land-use practices is essential for mitigating the combined effects of land use and climate change on the hydrology of the Dano basin. Implementing soil erosion management strategies, especially in proximity to farmlands and communities, is crucial. These measures aim to restrict surface runoff, enhancing soil infiltration capacity and ultimately replenishing groundwater resources. On the other hand, creating forests and grasslands is a crucial initiative toward mitigating the detrimental effects on water balance components brought on by future changes in land cover and climate.

4.0 CONCLUSIONS

In the semi-arid Dano catchment, water resource shortages are a significant concern due to climate and land-use changes impacting ecosystem services. To assist water resource managers in planning and adjusting to these changing conditions, the hydrological response of the Dano watershed to the conditional influence of these changes was quantified in this paper with the SWAT model and clearly shown in the surface flow, ground water/base flow (GWQ), lateral flow (LATQ), evapotranspiration (ET), and water yield. LULC changes reveal forest degradation, agricultural land expansion, settlement growth, and more stable grassland with savannah loss of about 8.18% under the Business-as-usual Scenario and likely increase by 2.13% in the afforestation scenario compared to a baseline condition. The simulated water balance components under LULC change slightly increased, except lateral flow, which decreased up to 1.46% under the afforestation scenario. Again, the influence of climate change is evident in the decline of mean annual precipitation by 20–22% as a consequence of global warming, marked by a substantial increase in mean annual temperatures of 1.50°C and 1.70°C under RCPs 4.5 and 8.5 scenarios, respectively. These projections indicate notable reductions in various hydrological parameters, including a significant decrease in surface runoff by 77%, evapotranspiration (ET) ranging from 8.6% to 11.1%, groundwater quality (GWQ) up to 90%, a 30% decrease in low-flow conditions (LATQ), and a substantial decline in water yield by 64% under both RCPs 4.5 and 8.5 scenarios.

Besides, the combined climate and LULC change effects on the hydrology of the catchment project overall decreasing water balance components by 2050. The predominant water loss from the catchment is primarily through evapotranspiration, underscoring the notable influence of soil moisture on the catchment's seasonal water balance. Additionally, the investigation indicated that the expansion of urban areas and croplands would marginally elevate streamflow. In summary, the overall decrease in freshwater availability, exacerbated to some extent by climate change-induced precipitation deficits, is further compounded by the expansion of agricultural activities. The study highlights significant correlation exists among climate patterns, streamflow, and human-related factors within the catchment. This linkage may elevate the vulnerability to increased occurrences of both droughts and floods. Hence, sustainable development goals 6, 13 & 15 can be attained by implementing sustainable land and water management practices such as afforestation, soil erosion control and water conservation, proposed to reduce the impact of changes in LULC and climate on the hydrology of Dano watershed.

Acknowledgement

The authors sincerely acknowledge the insightful comments and corrections of editors and reviewers. Also, my sincere gratitude goes to the institutions that gave free access to CORDEX climate models and the developers of the SWAT model. I also appreciate the United States Geological Survey (USGS) Department for the free access to satellite images and digital elevation models through their websites and applications. I appreciate the developers of the intensity analysis application and the Land Change Modeller team for making the model free to access.

Statements and Declarations

This study was performed within the West African Science Service Centre on Climate Change and Adaptive Land Use (WASCAL) Doctorate program, funded by the German Federal Ministry of Education and Research (BMBF).

Competing Interest

The authors declare there is no conflict of interest regarding the publication of this article.

REFERENCES

Adenle, A. A., Eckert, S., Adedeji, O. I., Ellison, D., & Speranza, C. I. (2020). Human-induced land degradation dominance in the Nigerian Guinea Savannah between 2003–2018. *Remote Sensing Applications: Society and Environment, 19*, 100360. https://doi.org/10.1016/j.rsase.2020.100360

Ahn, K. H., & Merwade, V. (2014). Quantifying the relative impact of climate and human activities on streamflow. *Journal of Hydrology, 515*, 257–266. https://doi.org/10.1016/j.jhydrol.2014.04.062

Akhoudas, C. H., et al. (2023). Isotopic evidence for an intensified hydrological cycle in the Indian sector of the Southern Ocean. *Nature Communications, 14*(1), 1–11. https://doi.org/10.1038/s41467-023-38425-5

Andreini, M., van de Giesen, N., van Edig, A., Fosu, M., & Andah, W. (2000). Volta Basin water balance. *ZEF Discussion Papers on Development Policy, 21*.

Arnold, J. G., et al. (2012). SWAT: Model use, calibration, and validation. *Transactions of the ASABE, 55*(4), 1491–1508.

Aston, P. J. (2002). Avoiding conflicts over Africa's water resources. *Ambio, 31*(3), 236–242. https://www.jstor.org/stable/4315243

Awotwi, A., Kumi, M., Pe, J., Yeboah, F., & Ik, N. (2015). Predicting hydrological response to climate change in the White Volta. *Earth Science & Climate Change, 6*(1), 1–7. https://doi.org/10.4172/2157-7617.1000249

Barry, B., Obuobie, E., Andreini, M., Andah, W., & Pluquet, M. (2005). *The Volta River Basin: Comprehensive assessment and management.* Water Report, 1–187.

Boretti, A., & Rosa, L. (2019). Reassessing the projections of the World Water Development Report. *npj Clean Water, 2*, 15. https://doi.org/10.1038/s41545-019-0039-9

Bossa, A., Diekkrüger, B., & Agbossou, E. (2014). Scenario-based impacts of land use and climate change on land and water degradation from the meso to regional scale. *Water, 6*(10), 3152–3181. https://doi.org/10.3390/w6103152

Bradshaw, C. J. A., Sodhi, N. S., Peh, K. S. H., & Brook, B. W. (2007). Global evidence that deforestation amplifies flood risk and severity in the developing world. *Global Change Biology, 13*(11), 2379–2395. https://doi.org/10.1111/j.1365-2486.2007.01446.x

Cannon, A. J., Sobie, S. R., & Murdock, T. Q. (2015). Bias correction of GCM precipitation by quantile mapping: How well do methods preserve changes in quantiles and extremes? *Journal of Climate, 28*(17), 6938–6959. https://doi.org/10.1175/JCLI-D-14-00754.1

Cohen, J. E. (2010). Population and climate change. *Proceedings of the American Philosophical Society, 154*(2), 158–182.

Cornelissen, T., Diekkrüger, B., & Giertz, S. (2013). A comparison of hydrological models for assessing the impact of land use and climate change on discharge in a tropical catchment. *Journal of Hydrology, 498*, 221–236. https://doi.org/10.1016/j.jhydrol.2013.06.016

Darko, D., Adjei, K. A., Appiah-Adjei, E. K., Obuobie, E., Asmah, R., & Odai, S. N. (2018). Simulation of climate characteristics and extremes of the Volta Basin using CCLM and RCA regional climate models. *Theoretical and Applied Climatology, 135*(1–2), 741–763. https://doi.org/10.1007/s00704-018-2485-6

Descroix, L., et al. (2009). Spatio-temporal variability of hydrological regimes around the boundaries between Sahelian and Sudanian areas of West Africa: A synthesis. *Journal of Hydrology, 375*, 90–102. https://doi.org/10.1016/j.jhydrol.2008.12.012

Dias, L. C. P., Macedo, M. N., Costa, M. H., Coe, M. T., & Neill, C. (2015). Effects of land cover change on evapotranspiration and streamflow of small catchments in the Upper Xingu River Basin, Central Brazil. *Journal of Hydrology: Regional Studies, 4*, 108–122. https://doi.org/10.1016/j.ejrh.2015.05.010

Duadze, S. E. K. (2004). *Land use and land cover study of the savannah ecosystem in the Upper West Region (Ghana) using remote sensing.* Göttingen: Cuvillier Verlag.

Fürst, C., & Flügel, W.-A. (2015). Assessing the impact of land-use changes on providing hydrological ecosystem functions and services – A case-study experience based conceptual framework. In *Ecosystem Services and River Basin Ecohydrology* (pp. 1–341). https://doi.org/10.1007/978-94-017-9846-4

Funk, C., et al. (2015). The climate hazards infrared precipitation with stations – A new environmental record for monitoring extremes. *Scientific Data, 2*, 66. https://doi.org/10.1038/sdata.2015.66

Forkuor, G., Hounkpatin, O. K. L., Welp, G., & Thiel, M. (2017). High resolution mapping of soil properties using remote sensing variables in south-western Burkina Faso: A comparison of machine learning and multiple linear regression models. *PLoS One, 12*(1), e0170478. https://doi.org/10.1371/journal.pone.0170478

Gasse, F. (2000). Hydrological changes in the African tropics since the Last Glacial Maximum. *Quaternary Science Reviews, 19*, 189–211.

Grillakis, M. G., Koutroulis, A. G., & Tsanis, I. K. (2011). Climate change impact on the hydrology of Spencer Creek watershed in Southern Ontario, Canada. *Journal of Hydrology, 409*(1–2), 1–19. https://doi.org/10.1016/j.jhydrol.2011.06.018

Gudmundsson, L., Bremnes, J. B., Haugen, J. E., & Engen-Skaugen, T. (2012). Technical note: Downscaling RCM precipitation to the station scale using statistical transformations – A comparison of methods. *Hydrology and Earth System Sciences, 16*(9), 3383–3390. https://doi.org/10.5194/hess-16-3383-2012

Haleem, K., et al. (2022). Hydrological impacts of climate and land-use change on flow regime variations in upper Indus basin. *Journal of Water and Climate Change, 13*(2), 758–770. https://doi.org/10.2166/wcc.2021.238

Hengl, T., et al. (2017). SoilGrids250m: Global gridded soil information based on machine learning. *PLoS One, 12*(2), e0169748. https://doi.org/10.1371/journal.pone.0169748

Hersbach, H., et al. (2020). The ERA5 global reanalysis. *Quarterly Journal of the Royal Meteorological Society, 146*(730), 1999–2049. https://doi.org/10.1002/qj.3803

Huntington, T. G. (2006). Evidence for intensification of the global water cycle: Review and synthesis. *Journal of Hydrology, 319*(1–4), 83–95. https://doi.org/10.1016/j.jhydrol.2005.07.003

Ibrahim, B., Karambiri, H., & Polcher, J. (2015). Hydrological impacts of the changes in simulated rainfall fields on Nakanbe Basin in Burkina Faso. *Climate, 3*, 442–458. https://doi.org/10.3390/cli3030442

INSD. (2020). *Annuaire statistique 2019.* Ouagadougou: Institut National de la Statistique et de la Démographie. Retrieved from https://www.insd.bf/contenu/pub_periodiques/annuaires_stat/annuaires_stat_nationaux_BF/Annuaire_Statistique_National_2019.pdf

IPCC. (2013). *The IPCC's fifth assessment report: What's in it for Africa?*

Executive summary. Retrieved from http://cdkn.org/wp-content/uploads/2014/04/J1731_CDKN_FifthAssesmentReport_WEB.pdf

IPCC. (2014). *Climate Change 2014: Mitigation of Climate Change. Assessment Report.* Geneva, Switzerland.

IPCC WGI Technical Support Unit. (2014). *Working Group I contribution to the IPCC fifth assessment report: Climate change 2013 – The physical science basis.* Final draft underlying scientific-technical assessment.

Knauer, K., Gessner, U., Fensholt, R., Forkuor, G., & Kuenzer, C. (2017). Monitoring agricultural expansion in Burkina Faso over 14 years with 30 m resolution time series: The role of population growth and implications for the environment. *Remote Sensing, 9*(2), 2132. https://doi.org/10.3390/rs9020132

Luhunga, P., Botai, J., & Kahimba, F. (2016). Evaluation of the performance of CORDEX regional climate models in simulating present climate conditions of Tanzania. *Journal of Southern Hemisphere Earth Systems Science, 66*(1), 32–54. https://doi.org/10.22499/3.6601.005

Mahe, G. (2006). The impacts of land-use/land-cover change and climate variability on the hydrology of the Sahel. In *Climate Variability and Change—Hydrological Impacts* (pp. 679–684). IAHS.

Moriasi, D. N., Arnold, J. G., Van Liew, M. W., Bingner, R. L., Harmel, R. D., & Veith, T. L. (2007). Model evaluation guidelines for systematic quantification of accuracy in watershed simulations. *Transactions of the ASABE, 50*(3), 885–900. https://doi.org/10.13031/2013.23153

Muhammed, H. H., Nasidi, N. M., & Wayayok, A. (2022). Impact of climate changes and land use/land cover changes on water resources in Malaysia. In A. M. F. Al-Quraishi, Y. T. Mustafa, & A. M. Negm (Eds.), *Environmental degradation in Asia* (pp. 321–340). Springer. https://doi.org/10.1007/978-3-031-12112-8_21

Mukhopadhaya, S. (2016). Land use and land cover change modelling using CA-Markov: Case study deforestation analysis of Doon Valley. *Journal of Agroecology and Natural Resource Management, 3*(1), 1–5.

Nazzal, J. M., El-Emary, I. M., & Najim, S. A. (2008). Multilayer perceptron neural network (MLPs) for analyzing the properties of Jordan oil shale. *World Applied Science Journal, 5*, 546–552.

Okafor, G. C., Annor, T., Odai, S. N., & Agyekum, J. (2019). Volta basin precipitation and temperature climatology: Evaluation of CORDEX-Africa regional climate model simulations. *Theoretical and Applied Climatology*, 1–25. https://doi.org/10.1007/s00704-018-2746-4

Okafor, G. C., Annor, T., Odai, S. N., & Larbi, I. (2019). Land use landcover change monitoring and projection in the Dano catchment, Southwest Burkina Faso. *International Journal of Advanced Remote Sensing and GIS, 9*(1), 3185–3204. https://doi.org/10.23953/cloud.ijarsg.445

Okafor, G. C., Larbi, I., Chukwuma, E. C., Nyamekye, C., Limantol, A. M., & Dotse, S. Q. (2021). Local climate change signals and changes in climate extremes in a typical Sahel catchment: The case of Dano catchment, Burkina Faso. *Environmental Challenges, 5*, 100285. https://doi.org/10.1016/j.envc.2021.100285

Pratap, S., & Markonis, Y. (2022). The response of the hydrological cycle to temperature changes in recent and distant climatic history. *Progress in Earth and Planetary Science, 9*(1). https://doi.org/10.1186/s40645-022-00489-0

Rameshwaran, P., Bell, V. A., Davies, H. N., & Kay, A. L. (2021). How might climate change affect river flows across West Africa? *Climatic Change, 169*(3–4), 1–27. https://doi.org/10.1007/s10584-021-03256-0

Roudier, P., Ducharne, A., & Feyen, L. (2014). Climate change impacts on runoff in West Africa: A review. *Hydrology and Earth System Sciences, 18*(7), 2789–2801. https://doi.org/10.5194/hess-18-2789-2014

Roy, T., He, X., Lin, P., Beck, H. E., Castro, C., & Wood, E. F. (2020). Global evaluation of seasonal precipitation and temperature forecasts from NMME. *Journal of Hydrometeorology, 21*(11), 2473–2486. https://doi.org/10.1175/JHM-D-19-0095.1

Sanogo, N. D. M., Dayamba, S. D., Renaud, F. G., & Feurer, M. (2022). From wooded savannah to farmland and settlement: Population growth, drought, energy needs and cotton price incentives driving changes in Wacoro, Mali. *Land, 11*(12), 2217. https://doi.org/10.3390/land11122117

Seibert, J., & Van Meerveld, I. (2016). Hydrological change modelling: Challenges and opportunities. *Hydrological Processes, 30*, 4966–4971. https://doi.org/10.1002/hyp.10999

Setegn, S. G., Srinivasan, R., & Dargahi, B. (2008). Hydrological modelling in the Lake Tana Basin, Ethiopia using SWAT model. *Open Hydrology Journal, 2*(1), 49–62. [https://doi.org/10.217

Sanogo, N. D. M., Dayamba, S. D., Renaud, F. G., & Feurer, M. (2022). From wooded savannah to farmland and settlement: Population growth, drought, energy needs and cotton price incentives driving changes in Wacoro, Mali. *Land, 11*(12), 2217. https://doi.org/10.3390/land11122117

Seibert, J., & Van Meerveld, I. (2016). Hydrological change modelling: Challenges and opportunities. *Hydrological Processes, 30*, 4966–4971. https://doi.org/10.1002/hyp.10999

Setegn, S. G., Srinivasan, R., & Dargahi, B. (2008). Hydrological modelling in the Lake Tana Basin, Ethiopia using SWAT model. *Open Hydrology Journal, 2*(1), 49–62. https://doi.org/10.2174/1874378100802010049

Shree, S., & Kumar, M. (2023). Assessment of the impact of land use and land cover change on hydrological components of the upper watershed of Subarnarekha River Basin, Jharkhand, India using SWAT model. *Water Conservation Science and Engineering, 8*, 50. https://doi.org/10.1007/s41101-023-00224-w

Sood, A., Muthuwatta, L., & McCartney, M. (2013). A SWAT evaluation of the effect of climate change on the hydrology of the Volta River Basin. *Water International, 38*(3), 297–311. https://doi.org/10.1080/02508060.2013.792404

Stephenson, J., Newman, K., & Mayhew, S. (2010). Population dynamics and climate change: What are the links? *Journal of Public Health, 32*(2), 150–156. https://doi.org/10.1093/pubmed/fdq038

Teutschbein, C., & Seibert, J. (2012). Bias correction of regional climate model simulations for hydrological climate-change impact studies: Review and evaluation of different methods. *Journal of Hydrology, 456–457*, 12–29. https://doi.org/10.1016/j.jhydrol.2012.05.052

Tripathi, H. G., Woollen, E. S., Carvalho, M., Parr, C. L., & Ryan, C. M. (2021). Agricultural expansion in African savannas: Effects on diversity and composition of trees and mammals. *Biodiversity and Conservation, 30*(11), 3279–3297. https://doi.org/10.1007/s10531-021-02249-w

Tucker, G. E., & Slingerland, R. (1997). Drainage basin responses to climate change. *Water Resources Research, 33*(8), 2031–2047. https://doi.org/10.1029/97WR00409

Wohl, E., Dwire, K., Sutfin, N., Polvi, L., & Bazan, R. (2012). Mechanisms of carbon storage in mountainous headwater rivers. *Nature Communications, 3*(1), 1263. https://doi.org/10.1038/ncomms2274

Winchell, M., Srinivasan, R., Di Luzio, M., & Arnold, J. (2010). *ArcSWAT interface for SWAT2009 user's guide.* College Station, TX: Texas A&M University.

Xavier, A. F. (2012). Improving water resources management through integration of community-based actions: The case of Black Volta Basin (Master's thesis). Kwame Nkrumah University of Science and Technology. Retrieved from http://ir.knust.edu.gh/bitstream/123456789/6552/1/Francis%20Anowie.pdf

Yan, F., et al. (2016). The effects of spatiotemporal changes in land degradation on ecosystem services values in Sanjiang Plain, China. *Remote Sensing, 8*(11), 917. https://doi.org/10.3390/rs8110917

Yang, D., Yang, Y., & Xia, J. (2021). Hydrological cycle and water resources in a changing world: A review. *Geography and Sustainability, 2*(2), 115–122. https://doi.org/10.1016/j.geosus.2021.05.003

Yang, Z., Zhang, Q., & Hao, X. (2016). Evapotranspiration trend and its relationship with precipitation over the Loess Plateau during the last three decades. *Advances in Meteorology, 2016*, 6809749. https://doi.org/10.1155/2016/6809749

Yira, Y., Diekkrüger, B., Steup, G., & Bossa, A. Y. (2016). Impact of climate change on water resources in a tropical West African catchment using an ensemble of climate simulations. *Journal of Hydrology, 537*, 187–199. https://doi.org/10.1016/j.jhydrol.2016.03.052

Zhang, J., Hu, Q., Wang, S., & Ai, M. (2017). Variation trend analysis of runoff and sediment time series based on the R/S analysis of simulated loess tilled slopes in the Loess Plateau, China. *Sustainability, 10*(1), 32. https://doi.org/10.3390/su10010032

Zhang, L., Nan, Z., Yu, W., & Ge, Y. (2015). Modeling land-use and land-cover change and hydrological responses under consistent climate change scenarios in the Heihe River Basin, China. *Water Resources Management, 29*(13), 4701–4717. https://doi.org/10.1007/s11269-015-1085-9

Xu, Y. P., Zhang, X., Ran, Q., & Tian, Y. (2013). Impact of climate change on hydrology of upper reaches of Qiantang River Basin, East China. *Journal of Hydrology, 483*, 51–60. https://doi.org/10.1016/j.jhydrol.2013.01.004